Steel and Composite Structures, *Vol. 15, No. 1 (2013) 1-14*
DOI: http://dx.doi.org/10.12989/scs.2013.15.1.001

Temperature on structural steelworks insulated by inorganic intumescent coating

J. Yoon Choi[1a] and Sengkwan Choi[*2]

[1] *Fire Safety Team, Division of Built Environment, Korea Conformity Laboratories, Seocho-dong, Seoul, 137-867, Republic of Korea*
[2] *School of the Built Environment, University of Ulster, Newtownabbey, BT37 0QB, UK*

(Received November 17, 2012, Revised May 24, 2013, Accepted May 28, 2013)

Abstract. Predicting the fire resistance of structures has been significantly advanced by full scale fire tests in conjunction with improved understanding of compartmental fire. Despite the progress, application of insulation is still required to parts of structural steelwork to achieve over 60 minutes of fire rating. It is now recognised that uncertainties on insulation properties hinder adaptation of performance based designs for different types of structures. Intumescent coating has recently appeared to be one of most popular insulation types for steel structures, but its design method remains to be confirmed by empirical data, as technical difficulties on the determination of the material properties at elevated temperatures exist. These need to take into account of further physiochemical transitions such as moving boundary and endothermic reaction. The impetus for this research is to investigate the applicability of the conventional differential equation solution which examines the temperature rise on coated steel members by an inorganic intumescent coating, provided that the temperature–dependent thermal/mechanical insulation properties are experimentally defined in lab scale tests.

Keywords: intumescent coating; temperature assessment; thermal property; steel structure

1. Introduction

Fire safety engineering has significantly progressed in recent decades. In particular, an enhanced understanding of in-fire performance of integrated structures, with advanced fire dynamic analyses to include the effect of a real fire severity, offers performance-based approaches to fire safety design (BSI 2003, Bailey 2003). The new design methods are able to allow structural steelwork to be partially protected with an optimum thickness of passive insulation, without compromising safety, but still achieving economic benefits. The overall reliability of the solution is based on an accurate prediction of temperature rise on insulated principal structural elements.

In the UK construction market, steel frame buildings have dominantly captured about 70% of non-residential multi-story buildings since 2005 (Steelconstruction.info 2012a). As the steel, like most construction materials, is inherently weak against fire, fire protection is typically required to maintain satisfactory functionality during the requisite fire resistance period. The insulation acts to

∗Corresponding author, Lecturer, Ph.D., E-mail: s.choi@ulster.ac.uk
[a] Ph.D., E-mail: j.yoon.choi@kcl.re.kr

 ISSN: 1229-9367 (Print), 1598-6233 (Online)

delay the time for steel to reach its failure temperature and subsequently allow fire fighters an appropriate period to control the fire. Although it is likely that a mixture of various types of fire protection materials are employed to secure building structures, intumescent coatings have an overall 70% share of the passive fire protection market (Steelconstruction.info 2012b). Fire protection typically accounts for around 10-15% of the total steel frame construction cost, therefore cannot be neglected.

Though intumescent coatings have been produced as a form of the structural fire protection for a considerable period of time, their use has dramatically increased over the past two decades due to their ability to provide equivalent protection with a decreased weight and thickness. Additional advantages such as speed of application, aesthetic appearance and easier protection of complex shapes are also present (Dowling *et al*. 2010). The new trend has typically been to use thin layered coatings which have a dry film thickness (d.f.t.) of less than 5mm and are primarily used internally. Intumescent coatings differ from conventional fire protection materials which are termed as reactive coatings. These break down and create a low conductivity char. This increases the longevity of the substrate in fire. In their dormant state intumescent coatings with a top coat may serve two functions, as a corrosion protectant and decoration (Allen 2001).

The intumescent steelwork coating is tested in accordance with BS 476 Pt20-21 (BSI 1987a, b) and ASFP Fire Protection for structural steel in buildings (ASFP 2010), otherwise known as Yellow book. ASFP (2010) describes in detail the test and assessment methods to approve 30, 60, 90 and 120 minutes' fire ratings upon application. Based on interpolated test data conducted according to the standard fire, the amount of reactive insulation applied for structures are currently assessed on performance based fire safety designs. The lack of reliable information on the time-dependent thermal/mechanical properties of reactive insulation is a major limitation for structural fire engineers to carry out non-linear numerical analyses of structures subjected to fire.

There have been comprehensive investigations carried out on the micro property aspects of the type of coating materials to understand reaction and thermal mechanisms (Anderson *et al*. 1985, Bourbigot *et al*. 1999, Staggs 2008, Omrane *et al*. 2007) and the macro aspects to be applied for structures (Zhang *et al*. 2012, Weijgert 2012). The complex nature of the material, i.e., expanding and endothermic reactions, create technical difficulties in defining its property in conjunction with stress induced detachment and crack. Further, there is no method to predict the performance of reactive insulation from tests carried out at laboratory scale to the larger tests at full furnace scale. These restraints result in creating a situation where instead of adapting a differential equation solution, the most common analytical method for board and spray insulations, the intumescent tends to be empirically defined by utilising analytic solutions, such as, numerical regression and graphical approach. This work intends to investigate the temperature rise on protected steel structures by using a partial differential equation, which is based on experimentally obtained properties of inorganic intumescent coating in small-scale tests.

2. Material properties of intumescent coating

The intumescent coating used for the presented work of this paper is an 'inorganic' type. Although its exact formulation is proprietary, the four main ingredients are known to consist of sodium silicate as an expanding agent, titanium dioxide, aluminum oxide and kaolinite as fillers. In comparison to a relatively common polymer based 'organic' intumescent coating, the type of insulation demonstrates distinctive thermal-mechanical characteristics in relation to the

intumescence process.

In the swelling procedure, ‘organic’ coatings produce a carbonic char layer which serves as a thermal insulation barrier but gradually ablates by further oxidation in air. On the contrary, inorganic coatings create a porous structure based on silicates with added fillers. It is identified that the expanded porous structure is more resilient to the high convectional flow presented in fire but adversely shrinks due to the phase change of the ingredients once exposed to heat beyond their melting temperatures. In terms of the decomposition gas, ‘inorganic’ coatings tend to mainly produce water vapours, due to the nature of the chemical makeup within the coating. When applied in confined environments with limited air circulation, it becomes critical to have non-toxic gas generated during intumescing.

In order to assess the temperature rise on insulated structural steelwork by using the partial differential method, thermo-physical properties of the coating should be continuously characterized with respect to temperature. It is particularly important in relation to the energy required for physiochemical changes to take place. It should be implemented for such aspects as latent heat, heat of decomposition and phase changes. This provides the rationale for the inorganic coating samples to be thermally treated at various targeted levels of temperatures and then the key properties, such as density, specific heat capacity and thermal diffusivity measured. The testing of the temperature took place on stable microstructural features. From the measurements, thermal conductivity was subsequently calculated at the designated levels of discrete temperature.

2.1 Sample preparation

An intumescent coating solution, commercially known as FC-Max, was employed to prepare the material test samples. An automatic film applicator, PA2101 Byk Gardner, was facilitated to create a uniform thickness of wet coated film. Each sample was then dried and stored under room conditions until no further weight decrease was monitored. Once the optimum dryness was achieved, the samples were heat treated by placing them in an electric furnace for 30 minutes at designated temperatures. The thermally expanded samples were subsequently used for the measurement of material properties.

2.2 Apparent density

Apparent density, which represents the overall density of the sample including internal pores, was obtained by measuring the weight of specimen in cubic centimetres volume. To minimize experimental errors, five replicas were tested at each temperature level. The average values of overall density with their standard deviation are shown at each temperature step in Fig. 1. In the figure, the density at 23°C, 2.08 g/cm^3, is acquired by only air-dried treatment without heat. At 200°C the density plummets to be 0.20 g/cm^3, approximately 10% of the dried only with further trivial fluctuation of 0.05 g/cm^3 observed up until 900°C. This immense density drop in the specific temperature zone indicates that the majority of intumescent behaviour appears to be complete below 200°C. The marginal increase of the density at 1000°C is originated from the melting of the ingredients.

2.3 Specific heat capacity

Specific heat capacity at a constant pressure (C_p) was measured by using a differential scanning

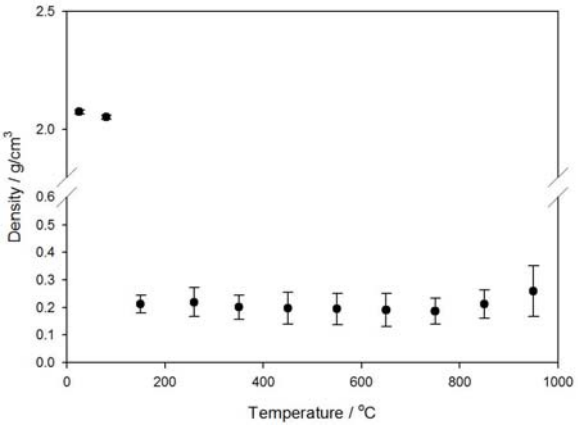

Fig. 1 Apparent density as a function of heat treatment temperature

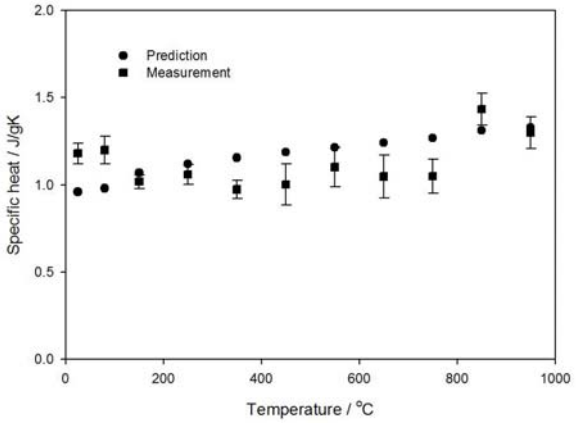

Fig. 2 Experimental and calculated specific heat capacity against heat treatment temperature

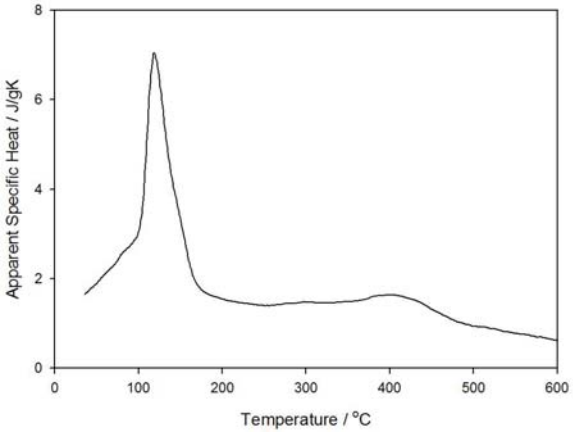

Fig. 3 Apparent specific heat measured from dried samples without heat treatment

calorimeter (DSC). A DSC 404 Netzsch was used complying with ISO 11357-4 (ISO 2001), with an increase in temperature of 10 K/min and a holding time of 15 minutes during the isothermal stages under nitrogen atmosphere. Fig. 2 represents the specific heat capacity change as a function of heat treated temperature. The trend demonstrates that the property is split into two temperature zones by the abrupt rise that occurred from 750°C to 850°C. However, within each zone, marginal variations occur in a range of 1.05 ± 0.05 J/gK and 1.35 ± 0.05 J/gK, respectively. As presented at Table 1, silicate is a substantial proportion of the composition and it undergoes a phase change around 850°C (Zotov 2002), which incurs the sudden ascent of measured specific heat to take place. For comparative purposes, a theoretical specific heat, $C_{p,}$ was estimated (Michot *et al*. 2008, ASTM 2004, Mitsuhashi and Watanabe 2000) and presented in Fig. 2. The formula used to calculate C_p is

$$C_p = \sum_i C_p F_i \tag{1}$$

where C_{pi} is the component specific heat capacity, F_i is the weight fraction of the component.

Table 1 Composition of inorganic materials within the solid contents of FC-Max (Comprising over 95% of solid contents of wet solution provided)

	Koalinite	Silicate	Alumina	Titanium oxide
Weight [%]	42.3	41.1	8.0	8.5

The difference of theoretical (calculated) and experimental (measured) values is 4-15%. This may be calculated from the empirical data from the industrial samples used for experiments and the limitation of its known composition. However, considering that there is 5% existing measurement uncertainty even for standard reference materials, this difference would imply that the experimental results contain an acceptable level of agreement with the calculated values.

In order to quantify the heat required for intumescence, the reaction energy and temperature range were measured from DSC experiments using only dried samples, prepared without the heat treatment process. The result is shown as a continuous form of apparent specific heat against temperature in Fig. 3.

2.4 Effective thermal conductivity

Using a laser flash apparatus, LFA 457 Netzsch, the thermal diffusivity was measured under the nitrogen atmosphere. The acquired data from experiments were parametrically analyzed by application of the Cape-Lehman model in conjunction with pulse correction. The thermal diffusivity assessed as a function of treated temperatures is presented in Fig. 4. There is a categorical exponential trend of increasing diffusivity with increasing temperature. Based on attained density, specific heat and thermal diffusivity values, an effective thermal conductivity, $K_{e(T)}$, was calculated as a function of temperature and plotted (See Fig. 4). The formula used to calculate effective thermal conductivity is

$$K_{e(T)} = \rho_{(T)} C_{p(T)} \alpha_{(T)} \tag{2}$$

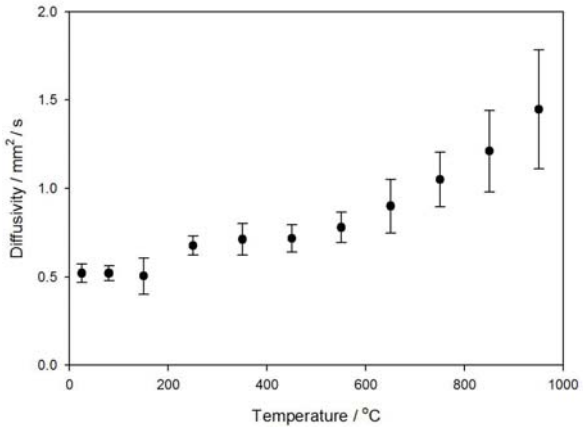

Fig. 4 Thermal diffusivity against temperature

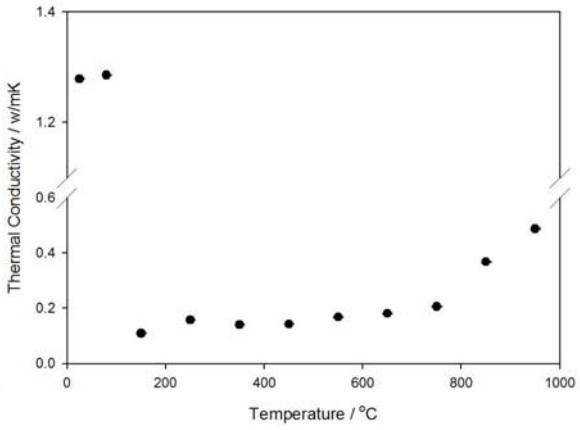

Fig. 5 Effective thermal conductivity against temperature

where $\rho_{(T)}$ is the temperature dependent density, $\alpha_{(T)}$ is the temperature dependent thermal diffusivity, $C_{p(T)}$ is the temperature dependent heat capacity.

The thermal conductivity rises significantly with increasing temperature. This is caused by the content of silicon oxides in the composition of kaolinite and silicates of which the inclination of thermal character was reported (Wall *et al*. 1979). The thermal conductivity presented at Fig. 5 is within 0.13-0.5 W/mK at the measured temperature range, which indicates the sample can act as a good thermal protection material. In comparison, that of coal ash is reported to be 0.4-1.1 W/mK between 200°C and 800°C. These substantially high figures are contributed to the action of very low porosities of coal ash that produce a result that lies between 0.29 and 0.48 (Rezaei 2000).

2.5 Simplified properties for analyses

Since there is not a single documented experimental method to determine continuous thermal properties such as thermal conductivity, apparent specific heat and density against temperatures, the curves, shown in Fig. 6, were constructed from the test results obtained at discrete temperature levels. These require continuous data for the prediction of temperature rise on the insulated structural steel detailed in Section 3. Due to the material decomposition and dehydration, the physiochemical transition was evolved at about 100°C to undergo the abrupt endothermic reaction. The reaction zone was implemented to be in a range of 90°C-130°C with an apparent peak of heat capacity 7000 J/kgK at 110°C. The activated thickness was measured at about 7-8 times of its dry film thickness.

3. Temperatures of insulated steelwork in fire

A program of experiments and analytical assessments of a series of indicative unloaded steel sections heated with/without insulation was carried out. The main aim was to quantify the

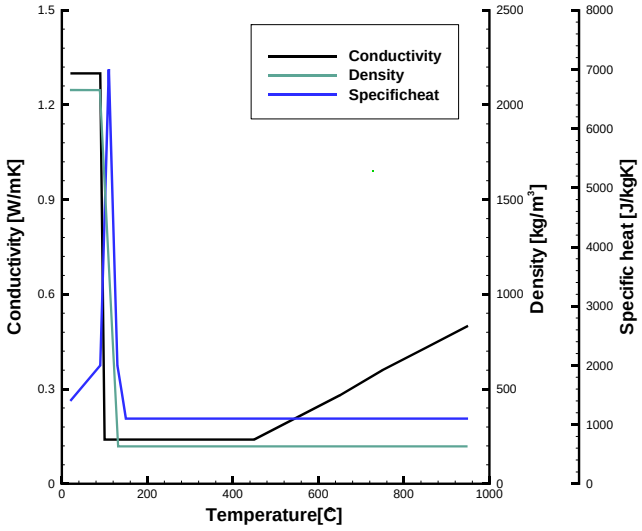

Fig. 6 Continuous properties against temperatures

sensitivity of furnace heat flux and investigate the direct applicability of measured temperature-dependent properties of intumescent coating for the calculation on the substrata's temperature rise. It also intended to clarify intrinsic uncertainties of insulation influencing its performance, such as geometry effect of substrata, and material degradation, once applied for structural members in a practical range.

3.1 Theoretical assessment

The methods to determine a temperature history of steel structures in furnaces have been thoroughly established (Wickstrom 1985a, b, 2005). As the thermal conductivity of steel is sufficiently high compared to the amount of exposed heat flux in the furnace or compartment fire, the Biot number for the structural elements is typically less than 0.1, which permits a lumped mass method to be employed for the section experiencing a uniform temperature distribution. Since the surrounding gas can be regarded to have higher temperatures, the governing equation for the 3D non-linear transient heat conduction of the unprotected cross-sections, described by Fourier's Law of heat transfer, can be simplified to be a 1D partial differential equation (BSI 2005a)

$$\Delta\theta_{a,t} = k_{sha}\left(\frac{1}{C_a\rho_a}\right)\left(\frac{A}{V}\right)\left(\dot{h}_{con}+\dot{h}_{rad}\right)\Delta t \tag{3}$$

where $\Delta\theta_{a,t}$ is the temperature increase of steel (K), Δt is the time interval (second), A/V is the section factor (1/m), c_a and ρ_a are the specific heat (J/kgK) and density (Kg/m^3) of steel, k_{sha} is a correction factor for the shadow effect, $\dot{h}_{con}$ and $\dot{h}_{rad}$ are the convective and radiative heat flux per unit area (W/m^2).

Once insulated, based on two additional hypotheses that no thermal resistance exists between the inner surface of the insulation and the contacted steel face and an exponential approximation represents the temperature variation across the insulation layer, the temperature rise on insulated steel section can be assessed by (BSI 2005a)

$$\Delta\theta_{a,t} = \left[\left(\frac{\lambda_p / d_p}{C_a\rho_a}\right)\left(\frac{A}{V}\right)\left(\frac{1}{1+\phi/3}\right)\left(\Delta\theta_t - \Delta\theta_{a,t}\right)\Delta t\right] - \left[\left(e^{\phi/10}-1\right)\Delta t\right] \tag{4}$$

with $\phi = (C_p\rho_p / C_a\rho_a)\, d_p\,(A_p V)$ and where C_p and ρ_p are the specific heat and density of insulation, d_p is the protection thickness, λ_p is the insulation thermal conductivity (W/mK), $\Delta\theta_t$ is the change of gas temperature (K), A_p is the area of the inner surface of the fire protection per unit length (m^2/m).

For unprotected I sections, a correction factor for shadow effect, k_{sha}, implemented through Eq. (3) replaces the section factor, A/V, with a shadow factor, 0.9 × [A/V]$_{b,}$ which is the 90% of the box value of the section factor (Wickstrom 2005). The modification was proposed by the opinion that the section contour can receive the energy at most though the smallest box profile surrounding the section. The reason is that the radiation emits only from the burner flame and the furnace walls in furnace tests. k_{sha} represents the view factors between internal concave surfaces of the section and the box outlines. An analogous heat transfer phenomenon can occur for insulated elements, in addition, the shadow factor can also be applicable to insulated structural steelwork (Eq. (4)). Therefore, in this work, the shadow effect was also included in the assessment of temperature rise on insulated sections.

Eq. (4), derived on the basis of the lumped capacitance method, is an adequate method for use within nonreactive coating which is only dependant on the temperature variation. Due to the reactive nature of intumescent coatings whose performance is additionally related to the heating regime, substrata profiles, protection thickness and compositions, it is often suited to be assessed with advanced numerical analysis techniques such as finite difference or finite element methods. However, as the continuous thermal properties of intumescent coating against temperature were experimentally obtained, the partial differential equation becomes applicable to estimate the heat transfer mechanism of the physiochemically non-linear insulation.

3.2 Experiments

Three groups of unloaded indicative fire tests, as described in Table 2, were conducted with a duration of one hour use of the standard ISO fire, using a medium research furnace in University of Ulster. UB 406 × 178 × 60, UC 254 × 254 × 89 and UB 610 × 305 × 238 sections were selected as for the substrate of each group and the section factor including the shadow effect for four sided

Table 2 Indicative test scheme

Section $0.9 \times [A/V]_b$	Unprotected	Target DFT of insulation		
		1.5 mm (Actual d.f.t.)	2.5 mm (Actual d.f.t.)	3.5 mm (Actual d.f.t.)
UB 406 × 178 × 60 [135 m^{-1}]	Specimen 1		Specimen 2 (2.7 mm)	Specimen 3 (3.3 mm)
UC 254 × 254 × 89 [80 m^{-1}]	Specimen 4	Specimen 5 (1.8 mm)	Specimen 6 (2.5 mm)	
UC 610 × 305 × 238 [55 m^{-1}]	Specimen 7	Specimen 8 (1.9 mm)	Specimen 9 (2.7 mm)	

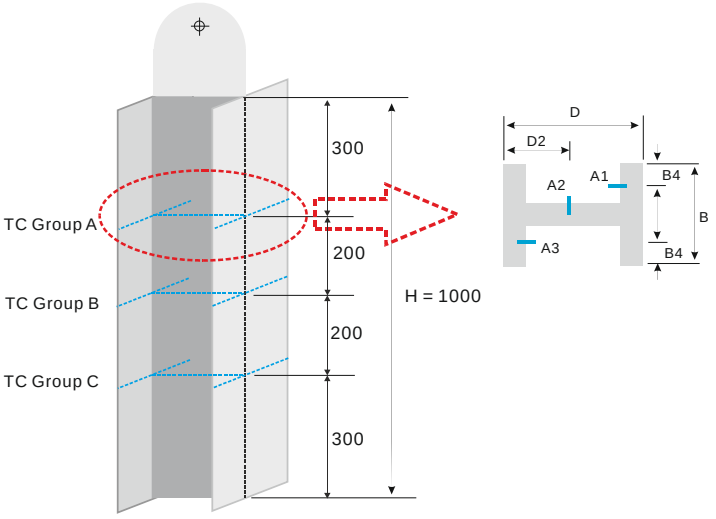

(a) UB and UC members (b) Thermocouple placement

Fig. 7 Detail of indicative test specimen

exposure was estimated by 0.9 $[A_p/V]_b$ to be 135/m, 80/m and 55/m, respectively. Each group was set to contain an unprotected and two insulated members with a target thickness of 1.5 mm, 2.5 mm or 3.5 mm. The actual d.f.t. of the applied insulation was measured to tolerate approximately ± 0.2 mm discrepancy from the target values. *K*-type thermocouples were installed at 3 positions across the Section and 3 locations along the member, as shown in Fig. 7, to record the temperature development in various parts of the section.

After the cooling off period, the post-test of specimens without/with 2.5 mm target d.f.t applied resulted in the sections being photographed, as illustrated in Fig. 8. In order to inspect the performance reservoir of insulation beyond the intended duration of fire, Specimens 2, 6 and 9 were tested for two hours, therefore causing further aging phenomenon of detachment and distortion of insulation to occur in Figs. 8 (d), (e) and (f).

(a) Specimen 1 (b) Specimen 4 (c) Specimen 7

(d) Specimen 2 (e) Specimen 6 (f) Specimen 9

Fig. 8 Temperature development of unprotected steel sections

In terms of the unprotected steel sections, the measured time-temperature curves of Specimen 1, 4 and 7 are plotted in Fig. 9. Fig. 9 also contains estimated values obtained by Eq. (3). As for the temperatures calculated, temperature-dependent thermal properties of steel were adapted in accordance with EC3 Pt1.2 (BSI 2005b). The design guidance offers thermal boundary setups used with the standard fire such that a convection coefficient of 25 KW/m^2 and a constant resultant emissivity of 0.7 are achieved. The temperature of bare steel was separately obtained along and across the flanges and webs, so the data measured contains up to 100°C of discrepancy. This is due to the effect of different element factors. Once they approach the gas temperature, the difference tends to diminish and the records converge to the estimation obtained by the section factor. The estimation is in good agreement with the experimental results for all of bare section cases indicated in Fig. 9. Though the convective coefficient and the resultant coefficient may vary against time in the course of fire, the constant values adapted result in reliable comparative outcomes for applications in the furnace.

For each insulated section in Table 2, the temperature variations, also measured at three positions along the web and six from the flange, are plotted in Fig. 10 for an hour of the standard fire. Due to the nature of intumescence, the coating often develops an uneven surface, crack and

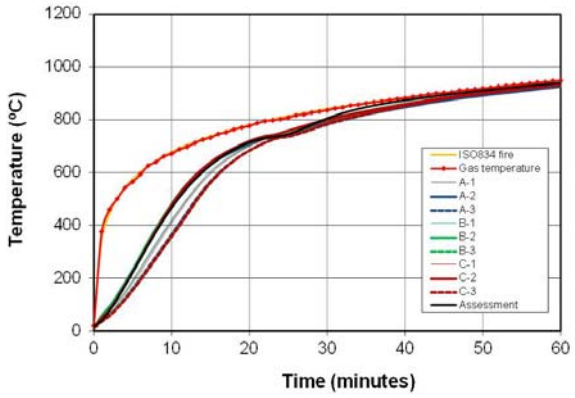

(a) Specimen 1

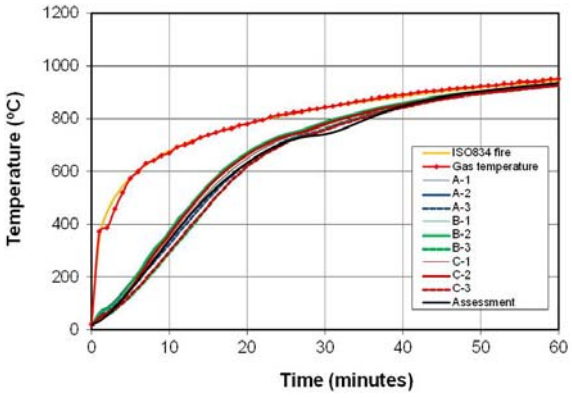

(b) Specimen 4

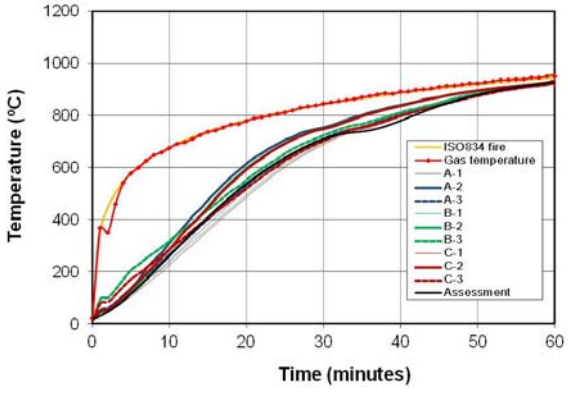

(c) Specimen 7

Fig. 9 Temperature development of unprotected steel sections

detachment, so the measured temperatures tend to scatter to create a band of 100-150°C towards the end of 60 minutes test. As the insulation remains intact to a greater extent in the concave area of the sections (web) shown in Fig. 8(f), the temperatures recorded from the part by A, B and C – 2 thermocouples create a consistent lower boundary for the temperatures in the band observed in all cases. With thicker insulation (Specimen 3 having 3.3 mm d.f.t), the insulation detachment at the outer surface of flanges tends to become worse and the temperature band extends over a range of 200°C. As a result of that, the flange temperatures of Specimen 3 (3.3 mm d.f.t.) exceed those of Specimen 2 (2.7 mm d.f.t.), though both used an identical size of substrata.

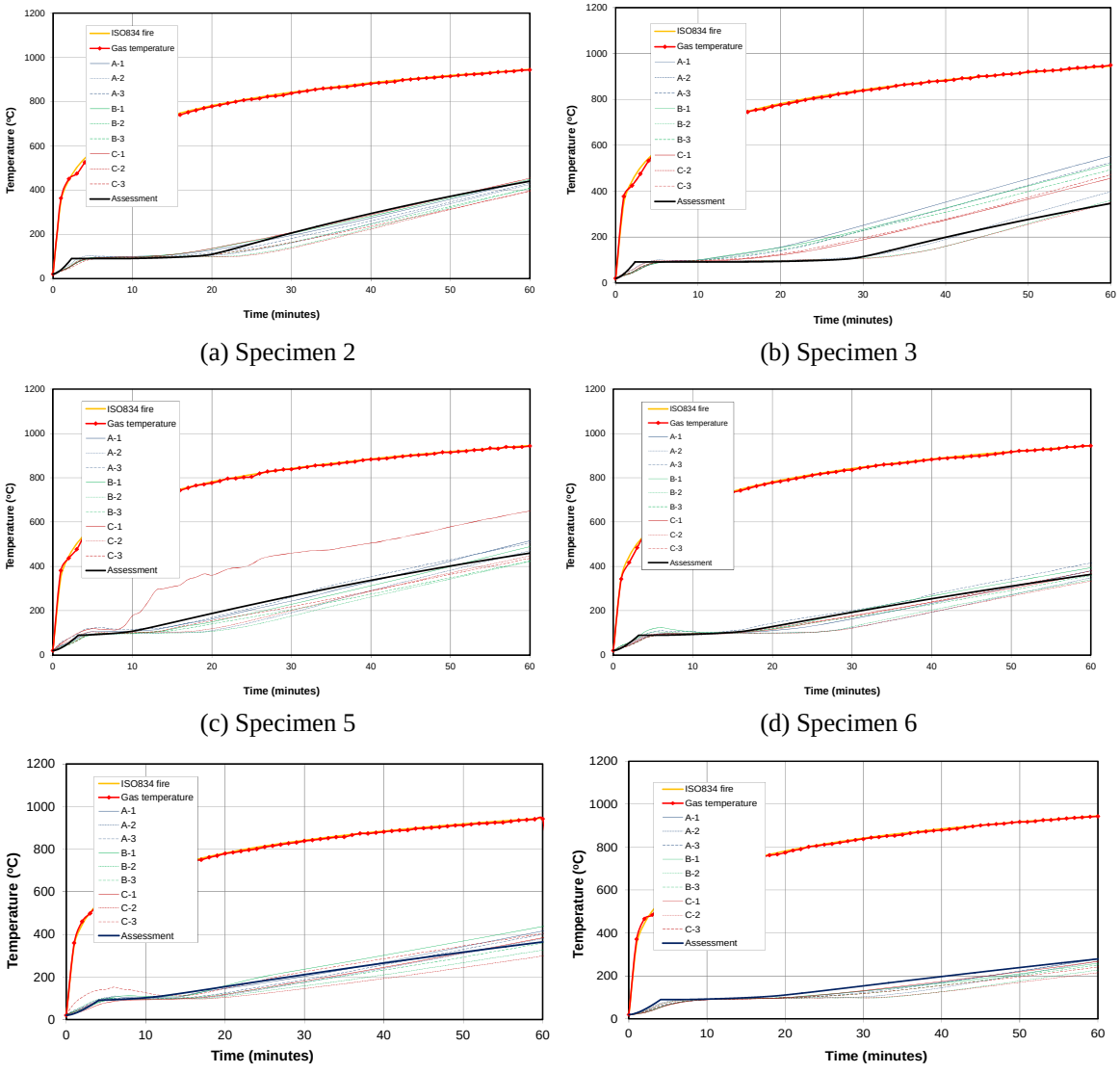

(a) Specimen 2

(b) Specimen 3

(c) Specimen 5

(d) Specimen 6

(e) Specimen 8

(f) Specimen 9

Fig. 10 Temperature development of insulated steel sections

In the insulated cases, the temperature growth contains a delay at 100°C, prompted by the dehydration and decomposition of the intumescence process. As the heat supplied is used to absorb the latent heat of water evaporation, the dwelling period is accordingly determined by the thickness of applied insulation. Based on the web temperatures recorded, approximately 7.2-7.6 minutes dwelling per 1.0 mm d.f.t. can be estimated with respect to the standard fire. As the water content of the insulation exists in the combination of free and chemically bonded conditions, the dwelling period estimation becomes complex and also it also relies on the imposed heat rate.

In terms of the temperature prediction of the substrate, the assessment was divided into two zones depending on the commencement at activation temperature, 90°C. During the zone up until 90°C, the temperature rise in substrata was obtained by Eq. (3) as if there was no protection applied. Then, after 90°C, 7.5 times of the actual d.f.t was assumed to be added to the outer surface to assess further temperature changes by Eq. (4). The temperature-dependent thermal properties of the insulation were given in Fig. 6. The outcomes are plotted in Fig. 10 in the form of recorded steel temperature histories. These results are compared with experimental data. With the exception of Specimen 3 in which early severe detachment and cracking was observed, the estimation correlates well with the steel temperatures, measured in a corresponding test not only in the delay period but also in the course of 60 minutes. The comparative assessment apparently demonstrates that the conventional partial differential equation can be adapted to assess the temperature rise on unloaded structural steelwork insulated by a reactive intumescent coating, provided that the material properties are adequately defined against time.

4. Conclusions

In the event of fire, the inorganic intumescent coating undergoes expansion and chemical changes to form a low thermal conductive media to protect the substrate from rapid growth of temperature. The use of intumescent coating practice for the protection of structures has been significantly enhanced the last decade, but its application has not been evaluated by heat transfer calculations. This project identifies a simplified way of estimating the temperature of insulated/unloaded steel members protected by intumescent material, based on lab-based material tests.

In order to define the thermal properties of the coating, measurements of density, specific heat and thermal diffusivity values were performed at discrete temperatures using lab-scale samples. The results indicate that effective thermal conductivity is about 0.11 W/mK, when thermally expanded at 150°C. It becomes equivalent to 8.5% of conductivity unexpanded at room temperature. This transition allows the coating to serve as an effective thermal barrier. However, due to the nature of the silicate compound, the expanded coating starts to melt at 750°C with a gradual increase in the conductivity to 0.5 W/mK at 950°C. Using dried only samples, the endothermic reaction was measured in a range from 90°C to 130°C with an apparent peak of heat capacity 7000 J/kgK at 110°C.

Based on the results of experimental measurement and interpolation of the thermal properties and geometrical changes of intumescent coating, it was demonstrated that the conventional partial differential equation can be utilised to predict the temperature rise on substrate protected by the reactive material. The assessment method proposed was also able to predict the dwelling period of temperatures, occurred due to the moisture evaporation, in relation to the applied d.f.t. and the section factor.

In comparison with the lab-scale results, further understanding was gained through the furnace tests in relation to the intumescence progress of inorganic intumescent coating. It indicates that this is significantly affected by the profile of substrata and the insulation thickness applied, in areas such as thermal stress crack and defect propagation over sharp concave edges. The performance of the coating seems not to improve with the applied thickness above the 2.5 mm level and also can be expected to vary according to the fire severity. Therefore, as this study has a number of fundamental limitations such as the use of standard fire and unloaded conditions, further test results need to be evaluated for its use in practice.

Acknowledgements

This project is funded by Korea Evaluation Institute of Industrial Technology through the Technology Innovation Program (Award No. 10041239): Fundamental technologies for development of nanoclay dispersed intumescent polymer composite in application for built environment and automobiles.

References

Allen, B. (2001), "Intumescent coating solutions in fire scenarios", *The 2nd International Conferences on Composites in Fire*, Newcastle upon Tyne, UK, September.

American Society for Testing and Materials (ASTM) (2004), *ASTM E1269-04*, Standard Test Method for Determining Specific Heat Capacity by Differential Scanning Calorimetry, West Conshohocken, PA.

Anderson, C.E., Dziuk, J., Mallow, W.A. and Buckmaster, J. (1985), "Intumescent reaction mechanism", *J. Fire Sci*., **3**(3), 161-194.

Association for Specialist Fire Protection (ASFP) (2010), *Fire protection for structural steel in buildings*, (4th Edition), UK.

Bailey, C.G. (2003), New Fire Design Method for Steel Frames with Composite Floor Slabs, FB5, BRE.

Bourbigot, S., Duquesne, S. and Leroy, J. (1999), "Modelling of heat transfer of a polypropylene-based intumescent system during combustion", *J. Fire Sci*., **17**(1), 42-56.

British Standards Institution (BSI) (2003), *PD7974* Application of fire safety engineering principles to the design of buildings: Part 3: Structural response and fire spread beyond the enclosure of origin, London.

British Standards Institution (BSI) (1987a), *BS476* Fire Tests on Building Materials and Structures: Part 20: Method for Determination of the Fire Resistance of Elements of Construction (General Principles), London.

British Standards Institution (BSI) (1987b), *BS476* Fire Tests on Building Materials and Structures: Part 21: Fire tests on building materials and structures - Methods for determination of the fire resistance of load bearing elements of construction, London.

British Standards Institution (BSI) (2005a), *Eurocode 4*: Design of Composite Steel and Concrete Structures – Pt. 1.2: General Rules-Structural Fire Design, BS EN 1994-1-2:2005, London.

British Standards Institution (BSI) (2005b), *Eurocode 3*: Design of Steel Structures – Part 1-2: General Rules-Structural Fire Design, BS EN 1993-1-2:2005, London.

Dowling, J.J., Newman, L.C. and Simms, W.I. (2010) *Structural Fire Design: Off-site Applied Thin Film Intumescent Coatings*, (2nd Edition), Steel Construction Institute, UK, pp. 160.

International Organization for Standardization (ISO) (2001), *ISO 11357-4*: 2001 Plastics-Differential scanning calorimeter (DSC) Part 4: Determination of specific heat capacity, Geneva.

Michot, A., Smith, D.S., Degot, S. and Gault, C. (2008), "Thermal conductivity and specific heat of kaolinite-Evolution with thermal treatment", *J. Eur. Ceram. Soc*., **28**(14), 2639-2644.

Mitsuhashi, T. and Watanabe, A. (2000), "Anomalies in heat capacity measurements of RuO_2 TiO_2 system", *J. Therm. Anal. Calorim.*, **60**(2), 683-689.
Omrane, A., Wang, Y.C., Goransson, U., Holmstedt, G. and Alden, M. (2007), "Intumescent coating surface temperature measurement in a cone calorimeter using laser-induced phosphorescence", *Fire Safety J.*, **42**(1), 68-74.
Rezaei, H.R., Gupta, R.P., Bryant, G.W., Hart, J.T., Liu, G.S., Bailey, C.W., Wall, T.F., Miyamae, S., Makino, K. and Endo, Y. (2000) "Thermal conductivity of coal ash and slags and models used", *Fuel*, **79**(13), 1697-1710.
Staggs, J.E.J. (2008), "A theoretical appraisal of the effectiveness of idealised ablative coatings for steel protection", *Fire Safety J.*, **43**(8), 618-629.
SteelConstruction.info (2012a), Cost of structural steelwork (online), [Accessed 1st Nov 2012], http://www.steelconstruction.info/Cost_of_structural_steelwork#Market_share_trend_in_uk_multi-storey_construction
SteelConstruction.info (2012b), Steel Insight – Cost planning through design process (online), [Accessed 1st Nov 2012], http://www.steelconstruction, info/File: Steel_Insight-3.pdf
Wall, T.F., Mai-Viet, T., Becker, H.B. and Gupta, R.P. (1979), "Fireside deposits and their effect on heat transfer in p.f. boilers: The emissivity and thermal conductivity of deposits and their components", *Proceedings Pulverized Coal firing - The Effects of Mineral Matter*, University of Newcastle, L8.1-16.
Weijgert, H. (2012), Assessment of intumescent coatings using the differential equation analysis (online) [Accessed 1st Nov 2012], http://fire-research.group.shef.ac.uk/steelinfire/downloads/HvdW06.pdf
Wickstrom, U. (1985a), Application of the Standard Fire Curve for Expressing Natural Fires for Design Purposes, Fire Safety: Science and Engineering, *ASTM STP 882*, 145-159.
Wickstrom, U. (1985b), "Temperature analysis of heavily insulated steel structures exposed to fire", *Fire Safety J.*, **9**(3), 281-285.
Wickstrom, U. (2005), "Comments on calculation of temperature in fire-exposed bare steel structures in prEN 1993-1-2: Eurocode 3 – design of steel structures – Part 1-2: General rules – structural fire design", *Fire Safety J.*, **40**(2), 191-192.
Zhang, Y., Wang, Y.C., Bailey, C.G. and Taylor, A.P. (2012), "Global modelling of fire protection performance of intumescent coating under different cone calorimeter heating conditions", *Fire Safety J.*, **50**, 51-62.
Zotov, N. (2002), "Heat capacity of sodium silicate glasses: Comparison of experiments with computer simulations", *J. Phys.: Condens. Matter*, **14**(45), 11655-11669.

CC